doi:10.3969/j.issn.1673-9736.2018.01.02
Article ID: 1673-9736(2018)01-0014-12

Geochronology and geochemistry of Baicaogou tuff in Yanji, NE China and its tectonic implications for Early Cretaceous

WANG Yingchao, SUN Fengyue*, LI Liang, XIN Wei, YAN Jiaming and TIAN Lidan

College of Earth Sciences, Jilin University, Changchun 130061, China

Abstract: The authors studied zircon U-Pb age and geochemical data of Baicaogou tuff in Yanji, Jilin Province. The results indicate that the rocks formed in Early Cretaceous (125.6 ± 2.3 Ma). Geochemically, these tuffs have high SiO_2 and total $Na_2O + K_2O$, low MgO and FeO, and they belong to metaluminous series, the rock are enriched in LREEs and LILEs, depleted in HREEs and HFSEs such as Nb, Ta, Ti, and P, exhibiting an affinity to I-type granite. All these characteristics implied that the volcanic rocks were derived from partial melting of lower crust. Combined with the geochronology and geochemical features of the coeval igneous rocks within NE China, it is concluded that Yanji area was in a back-arc extensional setting in response to the subduction of the Paleo-Pacific Plate beneath the Eurasian Plate.

Key words: Baicaogou tuff; zircon U-Pb age; I-type granite; subduction; Paleo-Pacific; Yanji

0 Introduction

Yanbian area is located in northeastern China and situated on the conjunction of Paleo-Asian ocean structural domain and Circum-Pacific structural domain (Zhang *et al.*, 2002). The large scale volcanic belt composed of Mesozoic volcanic rocks in Northeast China is an important part of the giant volcanic belt in the East Asian continent (Lin *et al.*, 1998). There are frequently intensive volcanic activities in Yanji area, but their stages and origin are unsure yet, due to the lack of precise geochronology and geochemistry analysis, which Lack of these essiential geological facts restricts the understanding of tectonic evolution in NE China. In this paper we focused on the Baicaogou tuff from Yanji area and examined them using LA-MC-ICPMS zircon U-Pb geochronology analysis in combination with whole-rock geochemistry analysis. Our results not only provided the zircon U-Pb age as evidence to precisely determine the age of volcanic rocks, but also provide evidence for the late Mesozoic volcanic activities and their tectonic significance in NE China.

1 Geological Background

NE China is located in the easternmost segment of the Central Asian Orogenic Belt (CAOB). Traditionally this area is regarded as an important junction of two different tectonic regimes, i.e. the EW-trending Paleo-Asian oceanic domain and the NNE-trending Paleo-Pacific domain. The study area, located in the conjunction of three massifs i.e. the Jiamusi massif, Xingkai massif and North China Craton, was situated to east of Dunhua-Mishang fault. (Fig. 1b) Over-

Received , accepted
Corresponding author(Email: sunfy@jlu.edu.cn)

all the tectonic evolution in the area during the Mesozoic, was dominated by the accretion of the East Asian continental margin in relation to the subduction of the Paleo-Pacific Plate, and the accretionary process accompanied by the formation of large volumes of arc rocks (both plutons and volcanic rocks) (Maruyama *et al.*,1997; Wu *et al.*, 2002; Xu *et al.*, 2009; Zhou *et al.*, 2014; Jahn *et al.*, 2015).

In the study area massive granitoids, occupying approximately ~70% of the exposed rocks in this region (JBGMR, 1988), were emplaced at two distinct stages, Late Triassic-Middle Jurassic (210–155 Ma) and Early Cretaceous (135–100 Ma). (Wu *et al.*, 2011) (Fig. 1a).

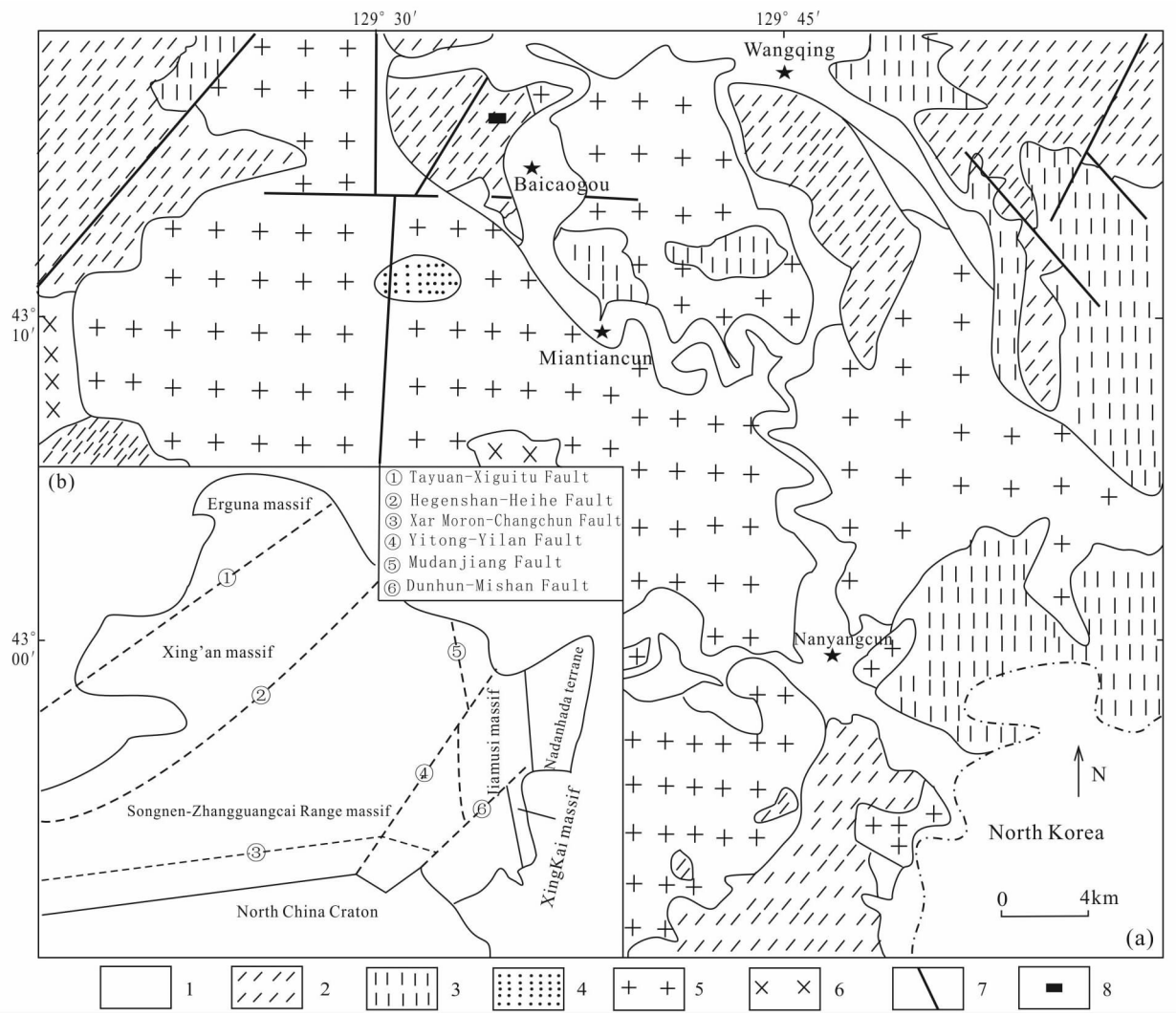

1-Quaternary ; 2-Mesozoic volcanic and volcaniclastic rocks; 3-Permian sedimentary; 4-Zhongping rock mass; 5-Miantian rock mass; 6-Other granites; 7-Fault; 8-sample Location

Fig. 1 Geological sketch map of Baicaoguo area

The samples were collected in northwestern Baicaogou, the Mesozoic volcanic and volcaniclastic rocks were exposed. The samples (Fig. 2) consisted of broken crystal fragments (quartz + k-plagioclase + biotite), volcanic ash, viroclasts, and accessory minerals such as Fe-Ti oxides, and zircon.

2 Analysis methods

2.1 LA-ICP-MS zircon U-Pb chronology

Zircons were extracted from Baicaogou tuff sam-

ples using heavy liquids and magnetic separation techniques in Langfang Regional Geological Survey, Heibei province, China. Zircon was carefully selected using binocular microscope and zircon of different characteristics was placed in the sticky glue, and fixed with transparent epoxy resin, the zircon surface was also polish. Transmitted light, reflected light and cathodoluminescence (CL) image (Fig. 3) were used before testing to define the best locations for U-Pb dating. LA-ICP-MS zircon U-Pb dating and trace elements analysis were all accomplished in State Key Laboratory of Continental Dynamicas, Northwest University. U-Th-Pb ratios and absolute abundant were determined by reference to multiple measurements of the

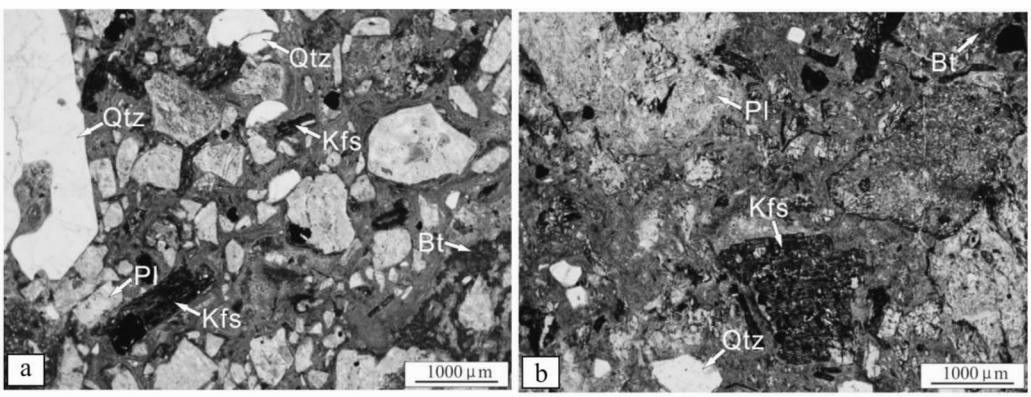

Qtz: Quartz; Kfs: K-feldspar; Pl: Plagioclase; Bt: Biotite.

Fig. 2 Microscopic photographs of Baicaogou tuff

zircon 91550 and NIST SR610 glass, and the detailed analytical method followed (Yuan *et al.*, 2003, 2004). Common Pb was regulated following Andersen (2002). The isotope ratios and contents were calculated by the ICP-MS-Data Cal program (Liu *et al.*, 2008). Age calculation and concordia diagram were obtained using Isoplot program (Ludwig, 2003).

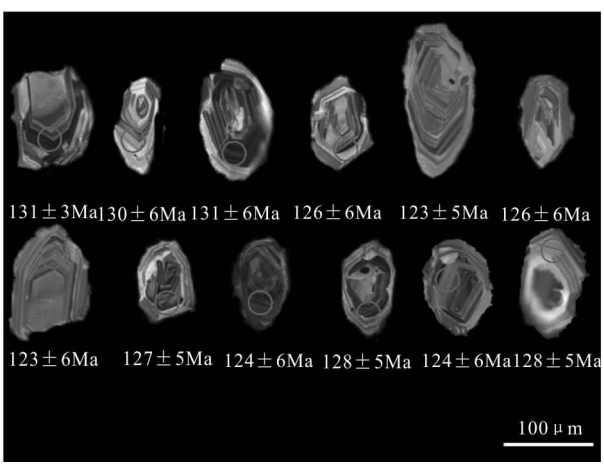

Fig. 3 CL image of zircon from Baicaogou tuff

2.2 Major and trace elements analysis

The samples which were used to analyze major and trace elements in College of Earth Sciences, Jilin University, were subsequently tested in Beijing Research Institute of Uranium Geology. Major elements were tested with Holland FHLISP PW2404 sequential scanning X-ray fluorescence spectrometer. Trace and rare-earth elements were tested and analyzed by ELEMENT Finnigan MAT inductively coupled plasma Mass spectrometry. Whereat, mass fraction of elements is less than 20 μg/g, and the error is within 10%. The final results errors are all within 5%.

3 Analysis result

3.1 LA-ICP-MS zircon U-Pd geochronology

Twenty-five samples were used to measure and test, and the results are listed in Table 1. According to these Cathodoluminescence (CL) images (Fig. 3), all of the zircons are euhedral or subhedral in shape with clear striped absorption and oscillatory zoning. And their Th/U ratios are between 0.74 and 1.74 ($\geqslant$ 0.4) (Belousova *et al.*,2002), indicating a magmatic origin for the zircons. The $^{206}Pb/^{238}U$ ages of twelve analytical spots range from 120 ± 5 Ma to 133 ± 6 Ma

(Supplementary Table 1), yielding a weighted mean $^{206}Pb/^{238}U$ age of 125.6 ± 2.3 Ma (Fig. 4), the formation time of the tuff is interpreted as 125.3 ± 1.2 Ma.

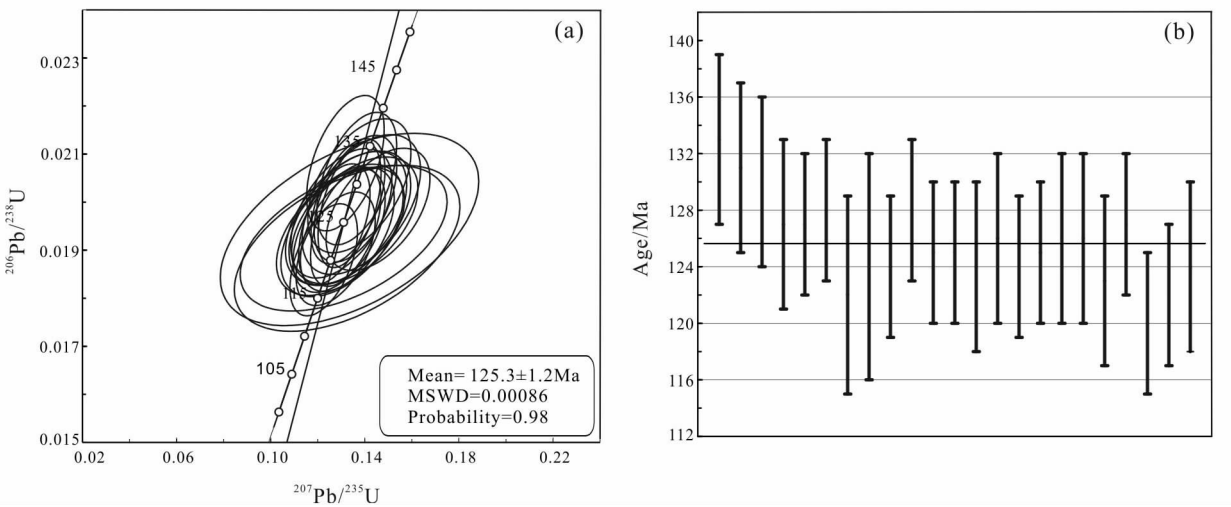

Fig. 4 U-Pb Concordia diagram and weighted average ages diagram

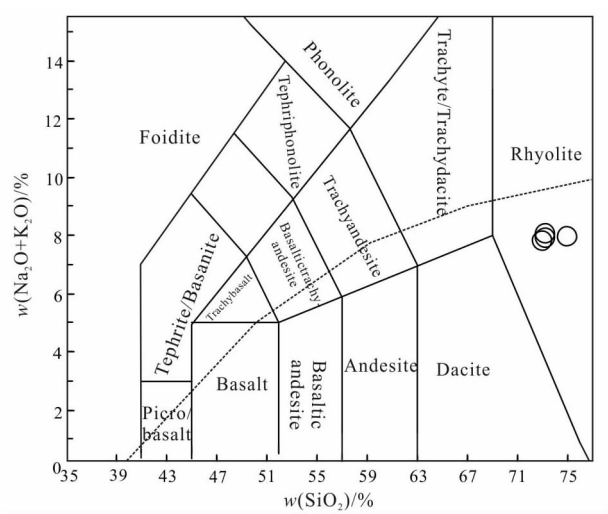

Fig. 5 Tas diagram of Baicaogou tuff

3.2 Major elements

Major and trace element data for the Baicaogou tuff are given in Table 2. Since the ignition loss (LOI) of the samples is too high (1.94% ~3.09%), certain correction was applied to the data. The Baicaogou tuffs have $w(SiO_2)$ =73.08%–75.10%. $w(Al_2O_3)$ =13.43%–14.27%, $w(MgO)$ =0.48%–0.79%, total $w(Fe_2O_3)$ =1.69%–2.36%, and total $w(Na_2O+K_2O)$ = 8.07%–7.82%. On a total alkali vs. silica (TAS) classification diagram of Wilson (1989), the data point fall in the rhyolite field (Fig. 5). Chemically, they belong to high-K calc-alkaline series (Fig. 6a; Peccerillo & Taylor, 1976). Their A/CNK ratios are in the range of 1.08% –1.13% showing weakly peraluminous characteristics (Fig. 6b; Maniar & Piccoli, 1989).

3.3 Rare earth elements and trace elements

On a chondrite-normalized REE diagram (Fig. 7a; Boynton, 1984), the Baicaogou tuffs are enriched in LREEs, depleted in HREEs with $(La/Yb)_N$ ratios of 8.70–13.72 and Eu/Eu^* of 0.62–0.68. On a PM-normalized trace element spider diagram (Fig. 8b; Sun & McDonough, 1989), the samples are enriched in LILEs (e.g., Sr, Rb, Ba, Th, U, and K) and depleted in HFSEs (e.g., Nb, Ta, Ti, and P).

4 Discussions

4.1 Petrogensis and magma source

The granites can be divided into three types i.e. A-type, I-type, and S-type, of which S-type granites are strongly peraluminous (A/CNK > 1.1) and generally contain aluminous minerals such as primary muscovite, cordierite and garnet (Chappell & White, 1974). But our samples are weakly peraluminous and no aluminous minerals are found, so these characteristics are not consistent with S-type granite. Comparing to the A-type granites, they have relatively low HFSE

Table 1 LA-MC-ICP-MS zircon U-Pb isotope dating

Samples	Pb	Th	U	U/Th	Pb^{207}/Pb^{206}		Pb^{207}/U^{235}		Pb^{206}/U^{238}		Pb^{207}/Pb^{206}		Pb^{207}/U^{235}		Pb^{206}/U^{238}		Pb^{208}/Th^{232}	
	10^{-6}	10^{-6}	10^{-6}		Ratio	1σ	Ratio	1σ	Ratio	1σ	Age/Ma	1σ	Age/Ma	1σ	Age/Ma	1σ	Age/Ma	1σ
BCG-N3-1	11.3	337	434	1.29	0.04590	0.00359	0.13176	0.01088	0.02081	0.00093	1	171	126	10	133	6	155	7
BCG-N3-2	15.0	491	611	1.24	0.04833	0.00375	0.13659	0.01121	0.02049	0.00091	116	174	130	10	131	6	148	7
BCG-N3-3	6.85	191	309	1.62	0.04908	0.00502	0.13768	0.01448	0.02034	0.00092	152	223	131	13	130	6	124	7
BCG-N3-4	12.3	469	553	1.18	0.05034	0.00597	0.13854	0.01662	0.01995	0.00096	211	253	132	15	127	6	135	8
BCG-N3-5	18.3	569	742	1.30	0.04853	0.00292	0.13351	0.00884	0.01994	0.00086	125	136	127	8	127	5	140	6
BCG-N3-6	6.99	201	285	1.42	0.04811	0.00353	0.13286	0.01039	0.02002	0.00086	105	165	127	9	128	5	144	6
BCG-N3-8	8.40	263	281	1.07	0.05043	0.01214	0.13249	0.03163	0.01904	0.00114	215	479	126	28	122	7	137	11
BCG-N3-9	4.81	132	224	1.693	0.04982	0.01371	0.13351	0.03627	0.01943	0.00132	187	539	127	32	124	8	80	14
BCG-N3-10	5.48	165	237	1.44	0.04948	0.00476	0.13259	0.01318	0.01943	0.00085	171	210	126	12	124	5	134	7
BCG-N3-11	16.0	702	554	0.79	0.04915	0.00403	0.13602	0.01161	0.02007	0.00087	155	181	130	10	128	5	149	6
BCG-N3-12	10.4	323	450	1.40	0.04715	0.00353	0.12705	0.01002	0.01954	0.00083	56	170	121	9	125	5	126	6
BCG-N3-13	10.1	325	424	1.31	0.04906	0.00346	0.13189	0.00988	0.01949	0.00082	151	157	126	9	125	5	131	6
BCG-N3-14	4.49	1308	206	1.59	0.04850	0.00666	0.12966	0.01797	0.01939	0.00088	124	295	124	16	124	6	142	8
BCG-N3-15	5.07	117	180	1.53	0.04900	0.00644	0.13292	0.01758	0.01967	0.00092	148	282	127	16	126	6	131	10
BCG-N3-17	10.2	336	448	1.33	0.04823	0.00473	0.12909	0.01294	0.01941	0.00085	111	216	123	12	124	5	132	7
BCG-N3-18	3.29	89.2	129	1.44	0.05019	0.00648	0.13577	0.01772	0.01962	0.00087	204	274	129	16	125	5	136	8
BCG-N3-19	17.4	546	755	1.38	0.04768	0.00515	0.12999	0.01420	0.01977	0.00089	83	239	124	13	126	6	126	7
BCG-N3-20	9.46	261	435	1.67	0.04900	0.00608	0.13279	0.01652	0.01966	0.00092	148	267	127	15	126	6	127	8
BCG-N3-21	3.43	129	147	1.14	0.04938	0.01099	0.13102	0.02903	0.01925	0.00100	166	451	125	26	123	6	130	10
BCG-N3-22	9.30	337	316	0.94	0.05325	0.00522	0.14564	0.01457	0.01985	0.00084	339	208	138	13	127	5	228	9
BCG-N3-23	13.3	672	498	0.74	0.04731	0.00350	0.12255	0.00947	0.01880	0.00077	64	168	117	9	120	5	127	5
BCG-N3-24	5.95	152	260	1.71	0.04866	0.00410	0.12760	0.01111	0.01903	0.00078	131	187	122	10	122	5	111	5
BCG-N3-25	12.1	430	493	1.15	0.04875	0.00642	0.13034	0.01716	0.01941	0.00091	136	283	124	15	124	6	126	7

Table 2 Major(%) and trace elements(10^{-6}) data

Sample	BCG-Y1	BCG-Y2	BCG-Y3	BCG-Y4	Sample	BCG-Y	BCG-Y2	BCG-Y3	BCG-Y4
SiO_2	73.64	71.05	70.87	71.08	In	0.01	0.02	0.02	0.02
Al_2O_3	13.17	13.83	13.69	13.85	Sb	0.50	0.56	0.83	0.64
Fe_2O_3	1.66	1.96	2.29	1.93	Cs	2.26	3.09	3.22	3.23
FeO	0.37	0.36	0.42	0.31	Ba	683.00	665.00	690.00	707.00
MgO	0.47	0.78	0.77	0.74	La	32.70	32.10	36.50	33.60
CaO	0.98	1.17	1.25	1.17	Ce	59.10	56.80	65.20	58.30
Na_2O	3.44	3.21	3.31	3.27	Pr	6.33	6.63	7.90	6.69
K_2O	4.35	4.46	4.27	4.56	Nd	21.50	23.80	29.00	24.10
MnO	0.06	0.09	0.11	0.10	Sm	3.40	3.71	4.78	3.83
TiO_2	0.20	0.24	0.24	0.24	Eu	0.66	0.80	1.03	0.76
P_2O_5	0.04	0.08	0.12	0.07	Gd	2.75	3.35	4.43	3.45
LOI	1.94	3.09	3.03	2.95	Tb	0.44	0.51	0.71	0.53
A/CNK	1.08	1.13	1.11	1.11	Dy	2.15	2.73	3.71	2.79
A/NK	1.27	1.37	1.36	1.34	Ho	0.45	0.57	0.76	0.57
TFe_2O_3	2.11	2.44	2.84	2.34	Er	1.34	1.72	2.44	1.77
TFeO	1.90	2.19	2.56	2.11	Tm	0.26	0.33	0.47	0.34
Mg#	20.21	26.91	23.57	26.45	Yb	1.71	2.20	3.01	2.29
Li	16.50	17.50	18.60	17.20	Lu	0.24	0.31	0.45	0.30
Be	1.66	1.99	2.20	1.50	W	0.72	1.00	1.28	1.12
Sc	2.65	3.22	3.6	3.43	Re	<0.002	<0.002	<0.002	<0.002
V	16.60	18.50	19.60	17.70	Tl	0.62	0.64	0.64	0.66
Cr	9.33	14.60	18.70	15.70	Pb	21.90	22.30	24.10	25.00
Co	2.70	4.12	4.91	3.76	Bi	0.03	0.89	1.34	0.77
Ni	4.96	6.44	6.88	6.37	Th	16.40	15.20	15.70	15.80
Cu	8.29	8.21	8.9	8.47	U	3.00	2.89	3.29	3.06
Zn	34.40	39.10	44.60	41.70	Nb	7.17	6.85	7.26	7.27
Ga	14.60	15.10	15.10	15.10	Ta	0.69	0.67	0.67	0.69
Rb	135.00	136.00	136.00	138.00	Zr	103.00	103.00	108.00	107.00
Sr	123.00	129.00	138.00	128.00	Hf	4.09	3.83	4.07	4.01
Y	13.00	18.40	27.40	19.00	$(La/Yb)_N$	13.25	10.57	9.04	10.57
Cd	0.04	0.04	0.04	0.04	Eu/Eu*	0.64	0.68	0.67	0.63

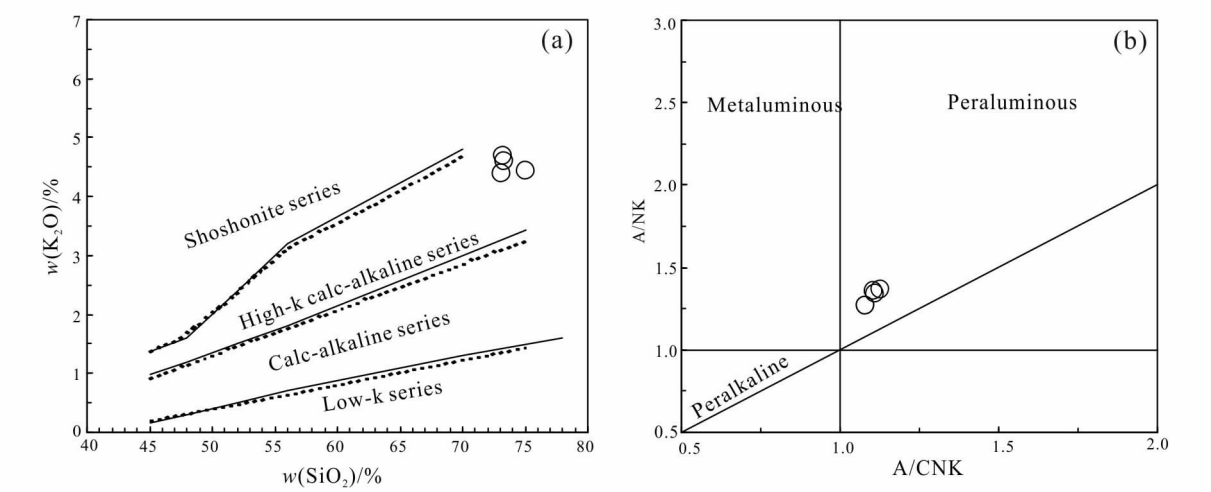

Fig. 6 Diagrams for SiO_2-K_2O (a) and A/CNK-A/NK (b) of Baicaogou tuff(b)

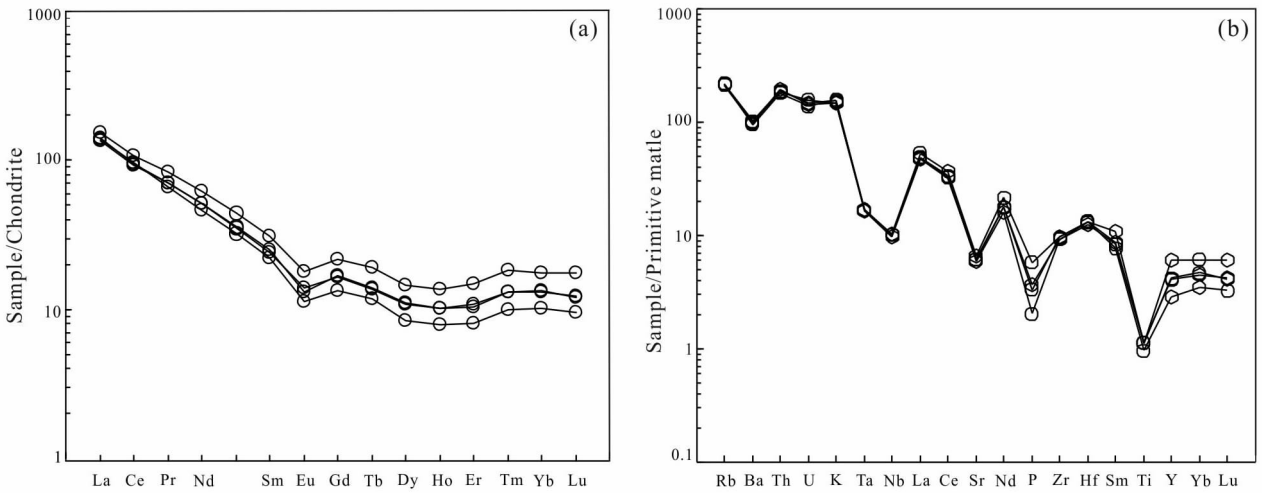

Fig. 7 Chondrite-normalized REE patterns (a) and primitive mantle-normalized trace element spider diagram (b) of Baicaogou tuff

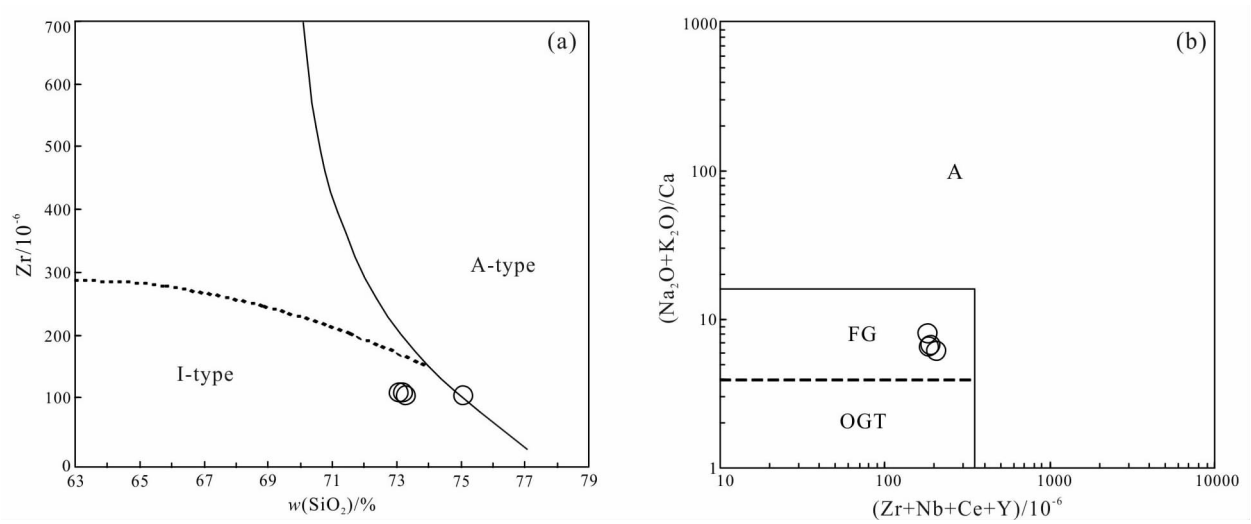

Fig. 8 Diagrams of SiO_2 vs. Zr (a) and (Zr + Nb + Ce + Y) vs. TFeO/MgO (b) for Baicaogou tuff

contents ($<350\times10^{-6}$). In the diagram of (Zr + Nb + Ce + Y) vs. TFeO/MgO and SiO_2 vs. Zr (Fig. 8) (Chappell and White, 1974), the samples resemble the characteristics of I type granites.

There are three presumptions about the petrogensis of magmatic rock in NE China: ①fractionation of basaltic magma (Yang *et al.*, 2006; Jahn *et al.*, 2000; Annen *et al.*, 2006). ②mixture of Mantle and crust magmas (Turner *et al.*, 1992; Han *et al.*, 1997). ③partial melting of crustal materials (Hildreth & Mtoorbath, 1988; Wu *et al.*, 2003). However, firstly, there are no synchronous basaltic magma activities in the Baicaogou area, indicating that the tuffs were not from fractionation of basaltic magma. Secondly mixing between the crust-derived melt and the mantle-derived melt will produce rocks with the presence of the mafic enclaves and inhomogeneous compositions, but samples have homogeneous geochemical characters, and no mafic enclaves exists either. Furthermore, there are no basic endmembers in the region which can mix with crust-derived melt. The most important addition of mantle derived materials, which should be enrich in contents of Ni, Cr and deleted in SiO_2 contents, but this is inconsistent with the samples of high SiO_2 (73.8 ~ 75.1%),

and low Cr ($9.33 \sim 18.7 \times 10^{-6}$), Ni ($6.37 \sim 4.96 \times 10^{-6}$). Furthermore ratios of Nb/Ta vary from 10.23 to 10.86, which resemble the crust ratio (average 8.3, Rudnick *et al.*, 2003) and differ from mantel ratio (average 17.5, Sun *et al.*, 1989). Ba/La ratios are between 18.90 to 21.04, they close to crust Ba/La ratio of 25 and be far away mantel Ba/La ratio of 9.6 (Weaver, 1991). So the tuffs derived from the crust.

Moreover, the samples are enriched in LILE (such as Rb, Th, U) but depleted in Nb and Ta. In addition it shows a negative Eu anomaly and relatively low Sr ($< 400 \times 10^{-6}$) (Fig. 8a), which requires melting of a source rock within the stability field of plagioclase (Wang *et al.*, 2016). It is therefore conclude that the source region of the granites is relatively shallow (<30 km). (Wang *et al.*, 2015).

High contents of SiO_2 indicate that the original magma is highly fractionated, negative anomaly of Eu, Ti and P indicate fractional crystallization of plagioclase, limonite, phosphate, rutile respectively.

In summary, the tuffs resemble I-type granites and were derived from partial melting of lower crust and have undergone significant crystallization differentiation.

4.2 Tectonic setting

Formation time of Baicaoguo tuff is in Early Cretaceous. There are four main viewpoints on the Mesozoic tectonic background in NE China as follow. ① Paleo-Asian oceanic slabs subduction (Windley *et al.*, 2007; Lehmann *et al.*, 2010). ②Mantel plume rise (Lin, 1998; Ge, 2000). ③Post orogenic extension after closure of the Mongolia-Okhotsk Ocean (Fan *et al.*, 2003). ④Paleo-Pacific plate subduction (Zhao *et al.*, 1998; Zhang *et al.*, 2008) Firstly, Previous studies have shown that the final closure of the Paleo-Asian Ocean between North China Craton and Siberian Craton along the Solonker-Xra Moron suture took place in the Late Permian (Ruzhentsev & Pospelov., 1992; Chen *et al.*, 2009 ; Xu *et al.*, 2013), which was followed by the post-orogenic adjustment in the Early Triassic (Dewey, 1988; Zhang *et al.*, 2008). But the formation time of Baicaogou tuff is in early Cretaceous, so the evolution of Paleo-Asian Ocean hardly influence tectonic evolution of the study area. Secondly, there are no reported symbolic products which represent mantel plume activities (Fan *et al.*, 2003), so the mantle plume rise viewpoint is given up. Thirdly, final closure of the ocean is suggested to have occurred sometime between the Late Jurassic (~155 Ma) and beginning of the Early Cretaceous (~120 Ma) (Zonenshain *et al.*, 1990; Kravchinsky *et al.*, 2002). And Mongolia-Okhotsk Ocean structural domain only affect western segment of Songliao Basin (Xu *et al.*, 2013), so it hardly affect the study area. Since the late Mesozoic, it is more obvious that NE China was significantly affected by subduction of the Paleo-Pacific plates (Zhao *et al.*, 1994; Maruyama *et al.*, 1997; Wu *et al.*, 2011). From Jurassic to Cretaceous, accretionary terranes and calc-alkaline I-type granitoids were widely developed along the eastern Asian continental margin, including NE China, Far East Russia and the Japan islands (Wickham *et al.*, 1995; Jahn *et al.*, 2004; Wu *et al.*, 2007; Sorokin *et al.*, 2010). Besides, the Rb, Th, U, K and LREE are enriched and Nb, Ta and Ti depleted, which suggest that the rocks originate in activity continental Margin (Gill, 1987). In (Yb + Nb)-Rb and (Yb-Ta)-Rb discriminate diagrams (Fig. 9), which exhibits that the samples all fall in volcanic arc granite (VAG) field. Combined with Early Cretaceous high-Mg diorites in the Yanji (Ma *et al.*, 2014), we conclude the tuffs are the products of Paleo-Pacific plates subduction.

The long-lasting subduction caused the initiation of extension on the back-arc side of the NE China (e.g., the Xing'an and Songliao areas) at 155–130 Ma (Fig. 10a). During the Early Cretaceous (130–110 Ma) (Fig. 10b), extensive back-arc extension occurred (Tatsumi and Kimura, 1991; Ge *et al.*, 2005 ; Ma *et al.*, 2013), as indicated by the formation of NNE-striking sedimentary basins (Liu *et al.*, 2010; Zhang *et al.*, 2011; Ge *et al.*, 2012), and the occurrence of immense volumes of I- and A-type granites (Wu *et al.*, 2000; Wu *et al.*, 2005; Jahn *et al.*, 2001; Jahn *et al.*,

2009). Volcanic rocks also occurred with the opening of the Songliao Basin, which constituted a typical bimodal igneous rock association (Zhang *et al.*, 2011; Xu *et al.*, 2013), suggesting an extensional environment induced by the roll-back of the Paleo-Pacific Plate. Extensive upwelling and injection of asthenospheric materials resulted in high-temperature conditions in the whole mantle wedge. During subduction of the Paleo-Pacific Plate beneath the Eurasian Plate, melting occurred in the mantle wedge and produced a large amount of basaltic magma. Then the basaltic magma ascended and underplated the lower crust, providing the necessary heat to cause partial melting of the lower crust, and the generation of voluminous granitic magma. Finally the granitic magma extruded out the surface, forming the tuff in the study area.

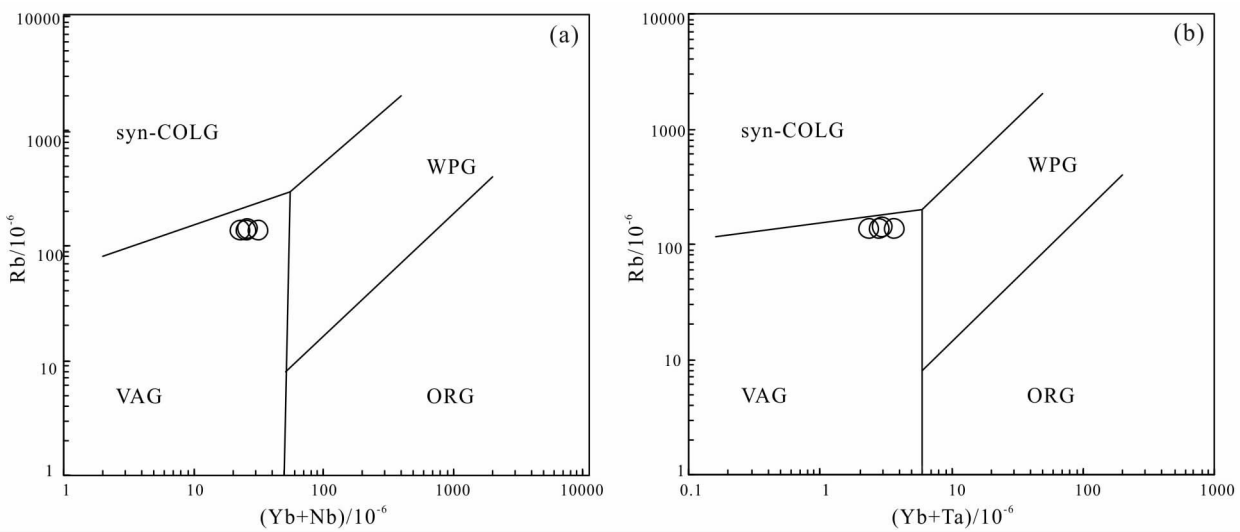

Fig. 9 Discriminations of (Yb + Nb)-Rb(a) and (Yb + Ta)-Rb(b) for Baicaogou tuff

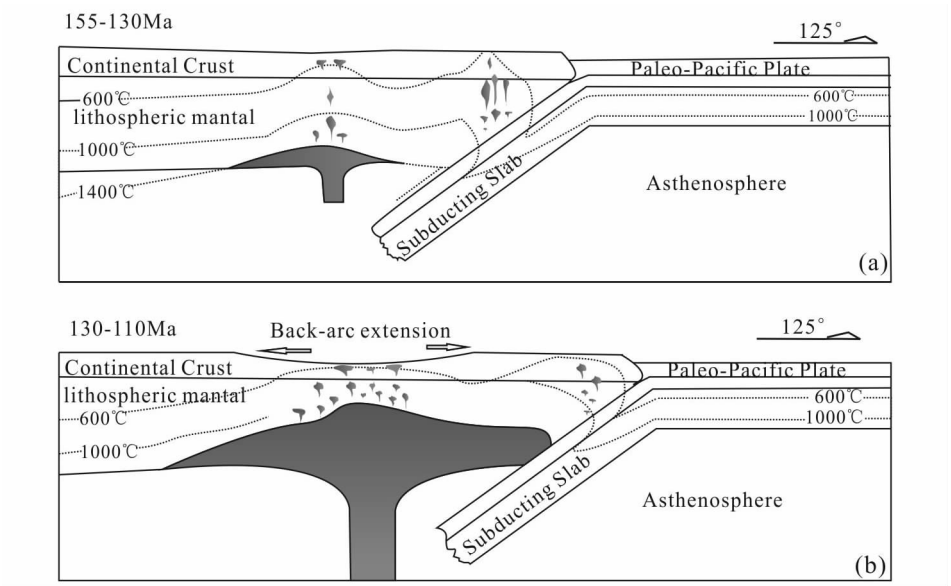

Fig. 10 Possible petrogenetic model of Baicaogou tuff in Yanji area, NE China

5 Conclusions

(1) Weighted mean age of Baicaogou tuff is 125.6 ± 2.3 Ma, corresponding to Early Cretaceous.

(2) Based on whole-rock chemical analyses and diagrams, it is concluded that the Baicaogou tuff is

similar to I-type granite and formed by partial melting of lower crust.

(3) During Early Cretaceous Yanji area was in a back-arc extension setting due to Paleo-Pacific plate subduction.

References

Anderson T. 2002. Correction of common lead in U-Pb analyses that donot report 204 Pb. *Chemical Geology*, **192**(1): 59-79.

Annen C, Blundy J D, Sparks R S J. 2006. The genesis of intermediate and silicic magmas in deep crustal hot zones. *Journal of Petrology*, **47**(3): 505-539.

Belousova E A, Griffin W L, O'Reilly S Y, *et al*. Igneous zircon : trace element composition as an indicatorof source rock type. *Contributions to Mineralogy and Petrology*, 2002, **143**(5): 602-622.

Chen B, Jahn B M, Wilde S, *et al*. 2000. Two contrasting Paleozoic magmatic belts in northern Inner Mongolia, China: petrogenesis and tectonic implications. *Tectonophysics*, **328**: 157-182

Chen B, Jahn B M, Tian W. 2009. Evolution of the Solonker suture zone: constraints from zircon U-Pb ages, Hf isotopic ratios and whole-rock Nd-Sr isotope compositions of subduction and collision-related magmas and forearc sediments. *Journal Of Asian Earth Sciences*, **34**: 245-257

Chappell B W, 1999. Aluminium saturation in I-type and S-type granites and the characterization of fractionated haplogranites. *Lithos*, **46**(9): 535-551.

Dewey J F. 1988. Extensional collapse of orogens. *Tectonics*, **7**: 1123-1139.

Fan W M, Guo F, Wang YJ, *et al*. 2003. Late Mesozoic calcalkaline volcanism of post-orogenic extension in the northern Da Hinggan Mountains, northeastern China. *Journal of Volcanology and Geothermal Research*, **121**(1): 115-135.

Gil F, Pla A. 2001. Biomarkers as biological indicators of xenobiotic exposure. *Toxicology science*, **21**: 245-255,

Ge W C, Lin Q, Sun D Y, *et al*. 2000. Geochemical research into origin of two types of Mesozoic rhyolites in Daxing'anling. *Earth Science*, **25**(2): 172-178. (in Chinese with English abstract)

Ge R F, Zhang Q L, Wang L S, *et al*. 2012. Late Mesozoic rift evolution and crustal extension in the central Songliao Basin, northeastern China: constraints from cross-section restoration and implications for lithospheric thinning Int. *Geology Research*, **54**:183-207.

Ge W C, Wu F Y, Zhou C Y, *et al*, 2005. Zircon U-Pb ages and its significance of the Mesozoic granites in the Wulanhaote region, central Da Hinggan Mountain. *Acta Petrol Sin*, **21**: 749-762. (in Chinese with English abstract)

Han B, Wang S, Jahn B, *et al*. 1997. Depleted-mantle sourcefor the Ulungur River A-type granites from North Xinjiang, China: geochemistry and Nd-Sr isotopic evidence, and implications for Phanerozoic crustal growth. *Chemical Geology*, **138**(3): 135-159.

Hildreth W, Moorbath S. 1988. Crustal contributions to arcmagmatism in the Andes of central Chile. *Contributions to Mineralogy and Petrology*, **98**(4): 455-489.

Jahn B M, Wu F Y, Chen B. 2000. Massive granitoid generation in Central Asia: Nd isotope evidence and implication for continental growth in the Phanerozoic. *Episodes*, **23**: 82-92.

Jahn B M R, Capdevila D Y, Liu A, *et al*. 2004. Sources of Phanerozoic granitoids in the transect Bayanhongor-Ulaan Baatar, Mongolia: geochemical and Nd isotopic evidence, and implications for Phanerozoic crustal growth. *Journal Of Asian Earth Sciences*, **23**: 629-653.

Jahn B. M, Wu F Y, Capdevila R, *et al*. 2001. Highly evolved juvenile granites with tetrad REE patterns: the Woduhe and Baerzhe granites from the Great Xing'an Mountain in NE China. *Lithos*, **59**: 171-198.

Jahn B M, Litvinovsky B A, Zanvilevich A N, *et al*. 2009. Peralkaline granitoid magmatism in the Mongolian-Transbaikalian belt: evolution, petrogenesis and tectonic significance. *Lithos*, **113**: 521-539.

Jilin Bureau of Geology and Mineral Resources (JBGMR). 1988. Regional geology of Jilin Province. Beijing: Geological Publishing House, 1-670. (in Chinese with English abstract)

Kravchinsky V A, Cogné J P, Harbert W P, *et al*. 2002. Evolution of the Mongol-Okhotsk Ocean as constrained by new palaeomagnetic data from the Mongol-Okhotsk suture zone, *Siberia Geophys*, **148**: 34-57.

Lehmann J, Schulmann K, Lexa O, *et al*. 2010. Structural constraints on the evolution of the Central Asian orogenic belt in SW Mongolia. *Life Sciences*, **310**: 575-628.

Lin Q, Ge W C, Sun Y, *et al*. 1998. Tectonic significance of Mesozoic volcanic rocks in Northeast China. *Geological Science*, **18**(2): 3-13.

Liu Y, Hu Z, Gao S, *et al*. 2008. In situ analysis of majorand trace elements of anhydrous minerals by LA-ICP-MS with-

out applying an internal standard. *Chemical Geology*, **257**(1): 34-43.

Ludwig K R. 2003. User's manual for Isoplot: a geochronological tool kit for Microsoft Execl. Berkeley: Berkeley Geochronology Center Special Publication, 4-1-70.

Lin Q, Ge W C, Sun D Y, *et al*. 1998. Tectonic significance of Mesozoic volcanic rocks in northeastern China. *Scientia Geological Sinica*, **33**(2): 129-139. (in Chinese with English abstract)

Liu S, Hu R Z, Gao S, *et al*. 2010. Zircon U-Pb age and Sr-Nd-Hf isotope geochemistry of Permian granodiorite and associated gabbro in the Songliao Block, NE China and implications for growth of juvenile crust. *Lithos*, **114**: 423-436.

Middlemost E A K. 1972. A simple classification of volcanic rocks. *Bulletin Volcanologique*, **36**: 382-397

Meng Q L, Zhou Y C, Chai S L. 2001. Porphyry hydrothermal vein type Cu-Au deposits, eastern Yanbian. Changchun: Jilin Science Technology Press, 1-163. (in Chinese)

Maniar P D, Piccoli P M. 1989. Tectonic discrimination of granitoids. *Geological Society of America Bulletin*, **101**: 635-643.

Maruyama S, Isozaki Y, Kimura G, *et al*. 1997. Paleogeographic maps of the Japanese Islands: plate tectonic synthesis from 750 Ma to the present. *Island Arc*, **6**: 121-142.

Ma X H, Chen B, Yang M C . 2013. Magma mixing origin for the Aolunhua porphyry related to Mo-Cu mineralization, eastern Central Asian Orogenic Belt. *Gondwana Research*, **24**: 1152-1171.

Ma X H, Cao R, Zhou Z H, *et al*. 2015. Early Cretaceous high-Mg diorites in the Yanji area, northeasternChina: Petrogenesis and tectonic implications. *Journal of Asian Earth Sciences*, **97**: 393-405.

Peccerillo A, Taylor S R, 1976. Geochemistry of Eocene calc-alkaline volcanic rocks from the Kastamonu area. *Contributions to Mineralogy & Petrology*, **58**(1): 63-81.

Rudnick R L, Cao S. 2003. Composition of the continental crust//Rudnick R L. (ed.) The crust treaties on geochemistry. Oxford: Elsevier Pergamon, 1-64.

Ruzhentsev S V, Pospelov I I. 1992. The south Mongolian Variscan fold system. *Geotectonics*, **26**: 383-395.

Sorokin A, Kotov A, Sal'nikova E B, *et al*. 2010. Ranitoids of the Tyrma-Bureya complex in the northern Bureya-Jiamusi superterrane of the Central Asian fold belt: age and geodynamic setting. *Russian Geology and Geophysics*, **51**(5): 563-571.

Sun S S, McDonough W F. 1989. Chemical and isotopic systematics of oceanic basalts: implition for mantle composition and processes. *Geoligical Socity Special Publication*, **42**(1): 313-345.

Turner S P, Foden J D, Morrison R S. 1992. Derivation of some A-type magmas by fractionation of basaltic magma: an example from the Padthaway Ridge, South Australia. *Lithos*, **28**(2): 151-179.

Tatsumi Y, Kimura N, 1991. Backarc extension versus continental breakup: petrological aspects for active rifting. *Tectonophysics*, **197**: 127-137.

Wu F Y, Yang J H, Lo C H, *et al*. 2007. The Heilongjiang Group: a Jurassic accretionary complex in the Jiamusi Massif at the western Pacific margin of northeastern China. *The Island Arc*, **16**: 156-172.

Wu F Y, Jahn B M, Wilde S, *et al*. 2000. Phanerozoic crustal growth: U-Pb and Sr-Nd isotopic evidence from the granites in northeastern China. *Tectonophysics*, **328**: 89-113.

Wu F Y, Lin J Q, Wilde S A, *et al*. 2005. Nature and significance of the Early Cretaceous giant igneous event in eastern China Earth Planet. *Earth Planetary Science Letters*, **233**: 103-119.

Wu F Y, Sun D Y, Ge W C, *et al*. 2011. Geochronology of the Phanerozoic granitoids in northeastern China. *Journal of Asian Earth Sciences*, **41**: 1-30.

Wu F Y, Sun D Y, Li H M, *et al*. 2002. A-type granites in northeastern China: age and geochemical constraints on their petrogenesis. *Chemical Geology*, **187**: 143-173.

Windley B F, Alexeiev D, Xiao W, *et al*. 2007. Tectonic models for accretion of the Central Asian Orogenic Belt. *Geological Societey*, **164**(12): 31-47.

Weaver B L. 1991. The origin of ocean island basalt end-member compositions: trace element and isotopic constraints. *Earth Planetary Science Letter*, **104**: 381-397.

Wickham S M, Litvinovsky B A, Zanvilevich A N, *et al*. 1995. Geochemical evolution of Phanerozoic magmatism in Transbaikalia, East Asia: a key constraint on the origin of K-rich silicic magmas and the process of cratonization. *Geophysics Research*, **100**: 15641-15654.

Xu B, Charvet J, Chen Y, *et al*. 2013. Middle Paleozoic convergent orogenic belts in western Inner Mongolia(China): framework, kinematics, geochronology and implications for tectonic evolution of the Central Asian Orogenic Belt . *Gondwana Research*, **23**(4): 1342-1364.

Yang J H, Wu F Y,Chung S L, *et al*. 2006. A hybrid origin-

for the Qianshan A-type granite, northeast China: geochemical and Sr-Nd-Hf isotopic evidence. *Lithos*, **89**(1): 89-106.

Yuan H L, Gao S, Liu X M, *et al*. 2004. Accurate U-Pb age and trace element determinations of zircon by laser ablationinductively coupled plasma-mass spectrometry. *Geostandards and Geoanalytical Research*, **28**(3): 353-370.

Yuan H L, Wu F Y, Gao S, *et al*. 2003. Zircon from Cenozoic intrusive body laser probe U-Pb time dating and rareearth element composition analysis. *Chinese Science Bulletin*, **48**(14): 1511-1520. (in Chinese with English abstract)

Zhao Y, Yang Z Y, Ma X H. 1994. Geotectonic transition from Paleo-Asian system and Paleo-Tethyan system to Paleo-Pacific active continental margin in eastern Asia. *Scientia Geological Sinica*, **29**: 105-119. (in Chinese with English abstract)

Zhang Y B. 2002. The isotopic geochronoligic frame of granitic magmatism in Yanbian area: doctor's degree thesis. Changchun: Jilin University. (in Chinese with English abstract)

Zhao H L, Deng J F, Chen F J, *et al*. 1998. Petrology of the Mesozoic volcanic rocks and the basin formation in the Northeast China. *Geoscience*, **12**(1): 56-62. (in Chinese with English abstract)

Zhou J B, Wilde S A, Zhang X Z, *et al*. 2009. The onset of Pacific margin accretion in NE China: evidence from the Heilongjiang high-pressure metamorphic belt. *Tectonophysics*, **478**: 230-246.

Zhang J H, Ge W C, Wu F Y, *et al*. 2008. Large-scale Early Cretaceous volcanic events in the northern GreatXing' an Range, Northeastern China. *Lithos*, **102**(1/2): 138-157.

Zonenshain L P, Kuzmin M I, Natapov L M. 1990. Geology of the USSR: a plate-tectonic synthesis. Washing D. C.: American Geophysical Union, 1-242

Zhang F Q, Chen H L, Yu X, *et al*. 2011. Early Cretaceous volcanism in the northern Songliao Basin, NE China, and its geodynamic implication. *Gondwana Research*, **19**: 163-176.

Zhang L C, Ying J F, Chen Z G, *et al*. 2008. Age and tectonic setting of Triassic basic volcanic rocks in southern Da Hinggan Range. *Acta Petrologica Sinica*, **24**: 911-920. (in Chinese with English abstract)